nature nanotechnology

INSIGHT | REVIEW ARTICLE

PUBLISHED ONLINE: 6 DECEMBER 2016 | DOI: 10.1038/NNANO.2010.207

The role of nanotechnology in the development of battery materials for electric vehicles

Jun Lu[1], Zonghai Chen[1], Zifeng Ma[2], Feng Pan[3]*, Larry A. Curtiss[4]* and Khalil Amine[1]*

A significant amount of battery research and development is underway, both in academia and industry, to meet the demand for electric vehicle applications. When it comes to designing and fabricating electrode materials, nanotechnology-based approaches have demonstrated numerous benefits for improved energy and power density, cyclability and safety. In this Review, we offer an overview of nanostructured materials that are either already commercialized or close to commercialization for hybrid electric vehicle applications, as well as those under development with the potential to meet the requirements for long-range electric vehicles.

A battery is an electrochemical device that stores electrical energy as chemical energy in its anode and cathode during the charging process, and when needed, releases the energy as electrical output during the discharge. An ideal battery is expected to have high specific energy, high power density, long cycle life, excellent abuse tolerance and low cost. Towards this goal, many battery systems have been actively pursued[1]. Among them, batteries based on Li-ion intercalation have attracted the most interest, because of their superior performance characteristics, namely, long cycle life, high energy and power densities, and no memory effect, since the introduction of commercial Li-ion batteries (LIBs) by Sony Inc. in 1991[2,3]. Other batteries based on chemical bonds, such as the Li–O_2, Li–S and Li–Se systems, have also been the focus of recent research due to their potentially much higher energy density[4,5]. Many advances in the battery technology could not have been possible without the development of new materials with desired properties based on the understanding and manipulating physicochemical processes on the 1 to 100 nm scale. For example, research on the latest anode and cathode materials for LIBs relies heavily on the use of nanocomposites and nanometre-thick coatings to optimize ionic and electronic conduction pathways, and block undesired, irreversible side reactions.

In this Review, we discuss recent advances in high-power and high-energy Li-based battery materials for electric vehicle (EV) applications enabled by nanotechnology. We focus on materials that are either already commercialized or close to commercialization as well as those under development. We first review the critical role of nanotechnology in enabling cathode and anode materials of LIBs. Then, we summarize the use of nanotechnology in other battery systems beyond Li-ion, including Li–S and Li–O_2, which we believe have the greatest potential to meet the high-energy requirement for EV applications.

Li-ion cathode materials

Since the introduction of LIBs into the market of portable electronics, the dominant cathode material has been $LiCoO_2$. However, due to its high cost and structural instability at high potential[6], this material has been ruled out as a suitable cathode material for EVs. In this section, we focus on how nanotechnology has enabled the development of other cathode materials, including olivines, doped lithium manganese oxide spinel and nickel-rich lithium-transition metal oxides.

Improving the transport properties of $LiFePO_4$. One of the first successful alternative cathodes for automobile applications has to be credited to nanostructured $LiFePO_4$. Although this olivine has a lower energy density than $LiCoO_2$, it exhibits significantly higher power density, longer lifetime and improved safety. Its potential was first recognized by John Goodenough[7], who initially suggested micrometre-sized $LiFePO_4$ for low-power applications. The low reversible capacity for micrometre-sized materials, especially at high current density, was associated with the slow movement in the Li_xFePO_4/Li_yFePO_4 ($0 < x < 0.1, 0.9 < y < 1$) boundary during the charge/discharge cycling[7]. Attracted by its favourable electrochemical potential, low toxicity, low cost and abundance of Fe, scientists put a significant amount of work into understanding what hinders high-rate performances (essential in hybrid EVs (HEVs)).

It is now widely believed that the covalent character of polyanion frameworks in $LiFePO_4$ is what limits electronic conductivity. To reduce the transport length of electrons, early research mostly focused on developing nanostructured $LiFePO_4$ (refs 8, 9). To enhance the efficiency of electron injection and removal and increase performances at a high current density, nanocoating $LiFePO_4$ with a conductive medium, such as carbon[10], conductive polymer[11] or conductive metal phosphides[12,13], has also been investigated. In addition, it was shown that the electronic conductivity of nanostructured $LiFePO_4$ could be increased by a factor of ~10^8 using non-stoichiometric solid-solution doping by metal cations supervalent to Li^+; this discovery resulted in an olivine materials capable of being charged/discharged at an extremely high current (up to 20 °C), for complete charge/discharge of the battery in less than 3 min (ref. 8).

Recent studies have also provided mechanistic insights on the Li^+ and electronic transport mechanisms in $LiFePO_4$. Figure 1a shows the projected crystal structure of $LiFePO_4$ in the (010) direction, displaying the diffusion channels for Li^+ in the (010) direction[14]. The [FeO_6] octahedrons are connected by sharing O corners to form a 2D network in the *bc* plane, while the [PO_4] tetrahedrons are physically separated (Fig. 1b) to connect adjunct [FeO_6] planes (Fig. 1c). Therefore, the diffusion of electrons in and out of $LiFePO_4$ relies on the [FeO_6] 2D framework.

Another limitation of $LiFePO_4$ is its poor percolation properties in 1D diffusion channels[15]. *Ab initio* calculations predicted a fast diffusion coefficient for Li^+ in 1D channels along the (010) direction; but, the occupation of Fe ions in Li sites (anti-site defects), as commonly found in $LiFePO_4$, can prevent Li^+ from hopping through the crystal structure. Lithium ions sitting in between a pair of defect sites are kinetically blocked (Fig. 1d, inset). Moreover, Li^+ diffusion along

[1]Chemical Sciences and Engineering Division, Argonne National Laboratory, Argonne, Illinois 60439, USA. [2]Institute of Electrochemical and Energy Technology, Department of Chemical Engineering, Shanghai Jiao Tong University, Shanghai 200240, China. [3]Materials, Peking University, Peking University Shenzhen Graduate School, Shenzhen 518055, China. [4]Material Science Division, Argonne National Laboratory, Argonne, Illinois 60439, USA. e-mail: panfeng@pkusz.edu.cn; curtiss@anl.gov; amine@anl.gov

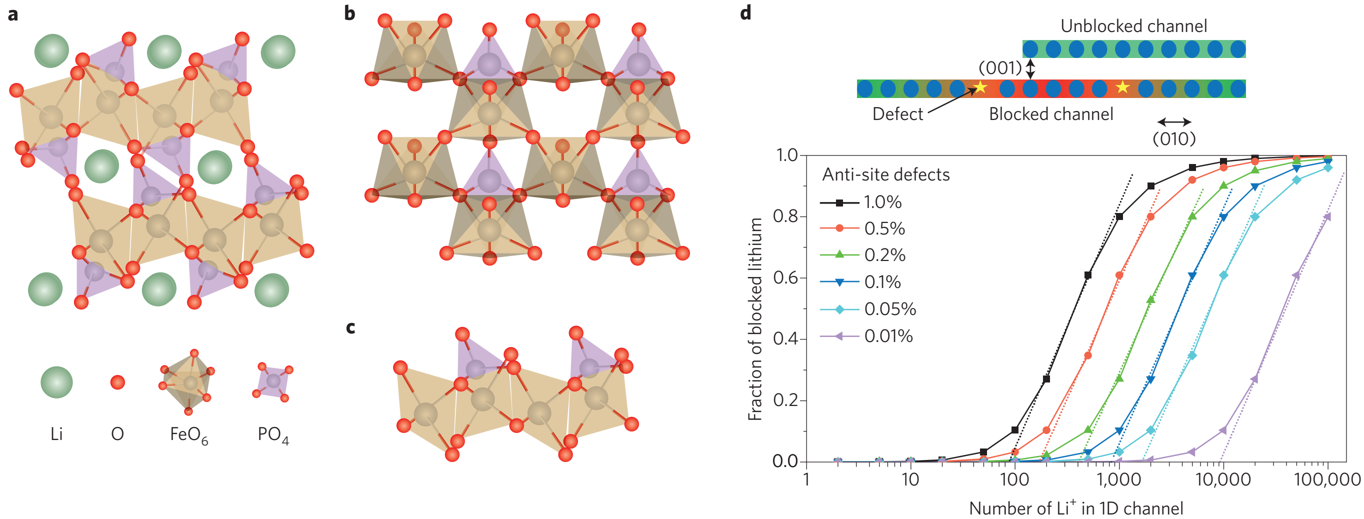

Figure 1 | Structure of $LiFePO_4$. a–d, 3D crystal structure (**a**), projection of 3D model on *ab* plane (**b**), projection of 3D model on *ac* plane (**c**) and theoretical prediction of blocked lithium in 1D channels by anti-site defects (**d**). The inset of panel **d** schematically shows blocked lithium ions in a blocked channel (red background sandwiched between two anti-site defects), which can diffuse into another (010) channel through the sluggish (001) channel. Panel **d** implies that particles with <50 nm in the (010) direction are free of impact from the anti-site defects, given the defect level is controlled at the 0.5% level (see the intercept between the red dotted line and the *x* axis).

the (001) direction is much slower and offers a sluggish way out for the blocked lithium, resulting in high potential polarization and low rate capability[16]. Figure 1d predicts the dependence of the amount of blocked Li in the 1D channel as a function of both the percentage of defects and the length of the channel. The reduction in the particle size of $LiFePO_4$ to a critical value can substantially reduce the amount of trapped Li and reduce the effect of the sluggish (001) diffusion channel for full utilization of the Li in the structure. As a result of these advances, nanostructured $LiFePO_4$ has been successfully deployed in HEVs and short-range EVs.

Suppressing manganese dissolution in $LiMn_2O_4$. Another class of cathode materials that has found successful applications in commercial automobiles (Chevy Volt and Nissan Leaf) is the doped lithium manganese oxide spinel, in which a percolated 3D diffusion network provides an efficient removal and insertion mechanisms of Li^+ during the charge/discharge process. One of the issues for $LiMn_2O_4$ spinel is the presence of a Jahn-Teller distortion of $[MnO_6]$ octahedrons at a low state of charge when Mn^{3+} is formed; the distortion is due to anisotropic breathing during charge/discharge cycling that results in structural instability. To mitigate the negative impact of the Jahn-Teller distortion, partial replacement of manganese with low valence state main group elements, such as lithium and aluminium, has been adopted. By reducing the amount of Mn^{3+}, this approach raises the average valence state of manganese at the end of discharge and substantially improves the cycle life of these spinels[17].

Another challenge is the dissolution of Mn^{2+} into the non-aqueous electrolyte, which eventually deposits on the surface of the graphitic anode and deteriorates the electrochemical performance[18,19]. Nanocoating with 10–20-nm-thick layers of various oxides or fluorides, such as ZrO_2 (refs 20,21), TiO_2 (refs 22,23), SiO_2 (ref. 21), Al_2O_3 (ref. 21) and AlF_3 (ref. 24), has been shown to protect the $LiMn_2O_4$ cathode from dissolution. In addition, functional electrolyte additives that form a nanopassivation layer at the electrode surface during the initial charge/discharge cycle were found to significantly improve the cycle life of this type of batteries[25,26].

Suppressing the chemical reactivity of $LiNi_{1-x-y}Mn_xCo_yO_2$. Unlike $LiCoO_2$ and $LiMn_2O_4$, in which only 0.5 Li atoms per transition metal atom deliver a reversible capacity of about 140 mAh g^{-1}, nickel-rich cathodes, $LiNi_{1-x-y}Mn_xCo_yO_2$ ($0 \le x, y, x + y \le 0.5$) can deliver a reversible capacity of about 200 mAh g^{-1} with an excellent capacity retention[27]. Delithiated nickel-rich cathodes are extremely reactive in non-aqueous electrolytes due to a substantial overlap between the 3*d* band of Ni and the 2*p* band of oxygen (Fig. 2)[28]. For this reason, nanoparticles and nanostructures of such cathode materials are generally undesired. Instead, nanocoatings have been used to reduce the exposed electrochemically active surface area and enhance cycle life.

Nickel-rich oxides have a tendency to lose oxygen at elevated temperatures and form rock-salt NiO on the surface. This leads to a degradation of the electrochemical performance of the final product[29]. To suppress the formation of NiO, material sintering needs to be carried out at a reduced temperature and/or oxygen-rich environment. This makes it difficult for commercial-scale synthesis of high-quality nickel-rich cathodes when the content of nickel is higher than 60%. Therefore, the main interest for large-scale deployment in EVs of these cathodes is focused on $LiNi_{0.5}Mn_{0.3}Co_{0.2}O_2$ and $LiNi_{0.6}Mn_{0.2}Co_{0.2}O_2$.

The chemical reaction between the charged nickel-rich cathode and the non-aqueous electrolyte leads to substantial reduction in reversible capacity (a loss of accessible lithium), a hike in the interfacial impedance (a loss of power density) and a severe reduction on the safety characteristics of the battery. A number of strategies have been studied to protect these nickel-rich cathodes from reacting with non-aqueous electrolytes (Fig. 3). For example, various nanocoatings, using oxides[30], fluorides[28] or phosphates[31], all serve well as a physical barrier between the nickel-rich cathode and the electrolyte, resulting in a significantly extended cycle life. This type of coating is generally composed of nanoparticles, typically ranging from 5 to 20 nm, which are formed in the liquid phase and deposited on the surface of the cathode material. These nanoparticles tend to aggregate, protecting some areas but leaving other areas uncoated[32] (Fig. 3a). To maximize protection, more nanoparticles can be deposited to form a complete coating layer[33] (Fig. 3b), which can be as thick as 100 nm.

Atomic layer deposition (ALD) is another method used to generate a sub-nanometre coating on the cathode surface[33] (Fig. 3c). It has been reported that a coating of three to five ALD cycles gives the best electrochemical performance[33]. However, it is still challenging to form a complete, conformal coating in three to five ALD cycles because the surface of nickel-rich cathodes lacks acidic groups that make ALD deposition effective.

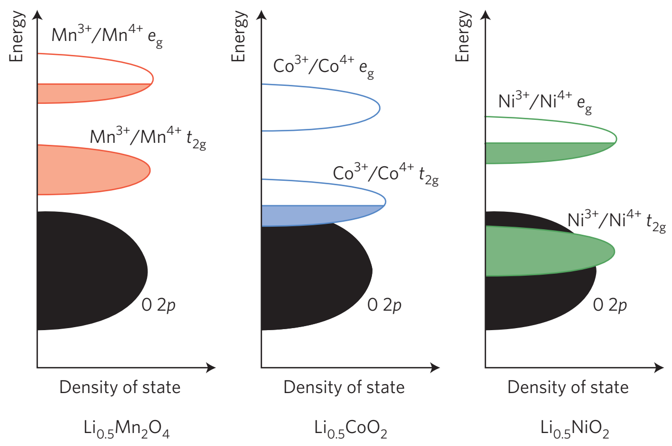

Figure 2 | Comparison of energy diagrams of various cathode materials. In the $LiCoO_2$ system, the t_{2g} band is completely filled and the e_g band is empty ($t_{2g}^6e_g^0$) with a low-spin Co^{3+} $3d^6$ configuration. During lithium extraction, electrons are removed from the t_{2g} band first. Since the t_{2g} band overlaps with the top of the O 2*p* band, deeper lithium extraction may result in a removal of electrons from the O 2*p* band, which will result in an oxidation of the O^{2-} ions and an ultimate loss of oxygen from the lattice. In contrast, the $LiNiO_2$ system with a low-spin Ni^{3+} $t_{2g}^6e_g^1$ configuration and the $Li_{1-x}Mn_2O_4$ system with a high-spin Mn^{3+} $t_{2g}^3e_g^1$ configuration involves the removal of electrons only from the e_g band. Figure adapted from ref. 28, Elsevier.

Alternatively, a core–shell nanostructure in which a manganese-rich shell protects the high capacity nickel-rich core has been investigated[34] (Fig. 3d). The manganese-rich phase has a lower reversible capacity but higher chemical stability towards non-aqueous electrolytes than the nickel-rich counterpart. Although the initial cycling performance improved, long-term cycling resulted in core–shell separation due to the mismatch of the lattice parameters of the two materials. To eliminate the sudden concentration change between the core and the shell, full concentration gradient cathode materials with a nanorod structure[28] have been developed (Fig. 3e)[35]. In a typical full concentration gradient cathode, the concentration of nickel continuously decreases from the centre towards the outer surface, while the concentration of protective material (manganese or cobalt) increases. In a full cell configuration, this material can deliver a reversible specific capacity of more than 200 mAh g^{-1} and an excellent capacity retention for 1,000 cycles.

It is important to note that there is a conceptual difference between the strategies shown in Fig. 3d,e (core–shell and full concentration gradient materials) and the development of unstructured materials. In unstructured materials (that is, without the core–shell or full concentration gradient concepts), the electrolyte can percolate into the porous structure of the particle, shortening the diffusion path of lithium ions during charge/discharge, leading to a better rate capability. For the core–shell and concentration gradient materials, the percolated voids in the particle can lead to a direct exposure of the nickel-rich core towards the non-aqueous electrolyte, with a detrimental impact on both the life and safety of the battery. It is, therefore, advantageous to synthesize compact nanostructured materials that minimize the amount of voids[36]. Finally, the development of more oxidation-resistant electrolytes[37] and electrolyte additives[38–40] that can form protective nanofilms on the surface of high-voltage cathodes will be beneficial for the adoption of nickel-rich cathodes for automobile applications.

Li-ion anode materials

LIB anode materials can be categorized into three groups: (1) insertion and de-insertion materials[41], including graphite[42] and titania[43],

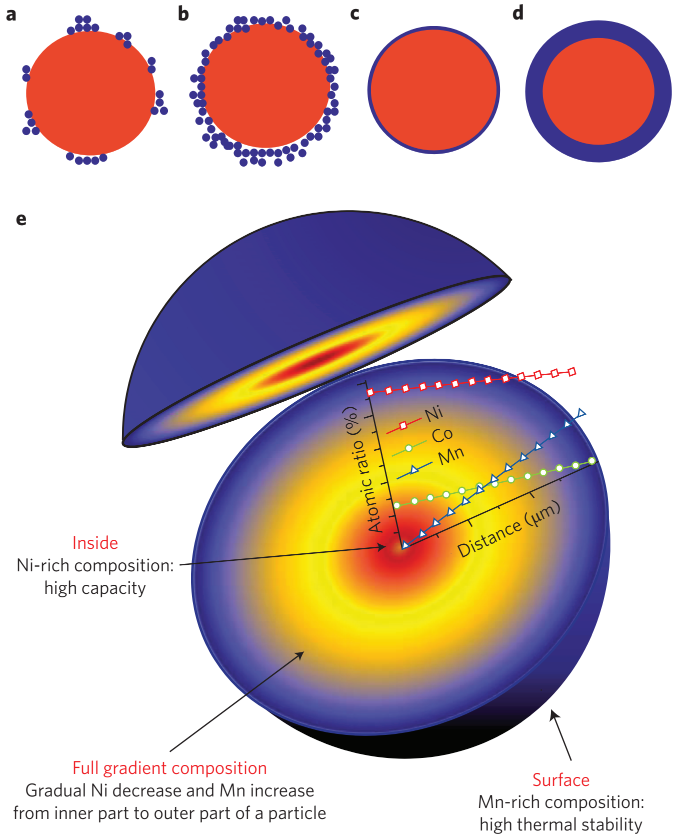

Figure 3 | Schematics of strategies to protect cathodes from reacting with non-aqueous electrolytes. a–e, Rough particulate coating (**a**), thin homogeneous coating (**b**), ultra-thin surface coating by atomic layer deposition (**c**), core–shell structure using manganese-rich shell to protect the nickel-rich core (**d**) and full concentration gradient cathodes with the concentration of nickel continuously decreasing from the centre to the surface (**e**). Panel **e** reproduced from ref. 35, NPG.

(2) alloy and de-alloy materials[44], such as tin and silicon alloys, and (3) conversion materials[45], such as metal oxides, metal sulfides, metal fluoride and metal phosphides. In this section, we focus on those materials that have been commercialized or are close to commercialization, especially for EV applications, and how nanotechnology has been critical in enabling the use of these materials.

Protecting graphite. Since the introduction of the first commercial LIBs, graphite has been the anode material of choice[41,42,46,47]. Its electrochemistry is based on the reversible intercalation/de-intercalation of Li ion into the host carbon inter-layers: $6C + xLi^+ + xe^- \leftrightarrow Li_xC_6$ $(0 < x < 1)$. The formation of LiC_6 during discharge yields a theoretical capacity of 372 mAh g^{-1}, which satisfies the demand of most current portable electronic devices. The electrochemical potential of Li-ion intercalation into the graphite host lies at about 0.15– .25 V vs Li^+/Li couple, making it a very attractive anode material. However, graphite also has some limitations. For instance, commonly used organic electrolytes (ethylene carbonate, diethylcarbonate, dimethylcarbonate, propylene carbonate) undergo irreversible reactions with lithiated graphite, although these electrolytes provide good Li^+ conductivity[48,49]. These side reactions include exfoliation of graphene sheets and reduction/decomposition of the electrolyte. One approach to mitigate this issue is growing a solid-electrolyte interface (SEI) as a nanosurface protection[50] by reducing ethylene carbonate molecules during the first cycle. The SEI helps to protect the graphite and prevents electrolyte decomposition, but it is not completely effective in passivating the anode surface. Therefore, improving protection of the graphite anode has long been actively pursued using strategies including surface oxidation[51] and protection with other nanocoatings[52].

There are primarily three types of nanocoatings currently pursued: amorphous carbon[53–55], metal and metal oxide[56,57] and polymer[58,59]. The amorphous carbon coating is usually deposited by thermal vapour deposition (TVD) with organic precursors at a high temperature[60], or mixing graphite with polymer precursors (for example, polyvinyl chloride, PVC) and annealing the mixture at 800–1,000 °C in an argon atmosphere[61]. These two approaches are favoured compared with chemical vapour deposition (CVD)[62,63] for large-scale industrial implementation due to lower cost. Metal and metal oxide coatings, in the order of 10–20 nm, on a graphite surface[56,57,64] efficiently minimizes side reactions with the electrolyte at the interface and improves the rate performance of the cell. There has been a large library of materials explored for this purpose, including Cu, Ni, Sn, Zn, Al, Ag, TiO_2, MoO_3 and SnO_2 (refs 56,57,64). Many of these nanocoatings are fabricated using a wet-chemistry approach (electrolysis plating)[64], while others are applied using vacuum deposition techniques, including CVD and ALD[63]. There are also several polymers employed for the same purpose, for instance, polyurea, polypyrrole, PVC, polyaniline and polythiophene[58,59,65–67]. All these approaches are promising for EV application considering the effective protection of graphite they provide, as well as their potential for scale-up processing.

Improving power using nanostructured lithium titanates and titanium oxides. Lithium titanate ($Li_4Ti_5O_{12}$, LTO) spinel has proven to be a viable alternative to graphite as anode material because of its outstanding safety characteristics[43]. Li ions diffuse into the LTO lattice and occupy the free octahedral sites. Such insertion/de-insertion brings no strain to the host and minimum volumetric change, a very attractive property in anode materials. Moreover, the relatively high electrochemical potential of LTO for lithium insertion (~1.55 V vs. Li^+/Li) renders it inert to the organic electrolyte. Most importantly, compared with graphite, LTO is an intrinsically safer anode material, with minimal irreversible capacity loss during cycling. Unfortunately, due to its unique crystal structure and large electronic bandgap (2–3 eV)[68], LTO is intrinsically limited in two aspects: (1) it has a relatively small theoretical capacity (175 mAh g^{-1}) compared with graphite (372 mAh g^{-1}) and (2) it has a low electronic and Li-ion conductivity (3×10^{-8} S cm^{-1} and 1×10^{-12}–1×10^{-13} S cm^{-1} at 300 K, respectively) compared with graphite (10^{-4} S cm^{-1} and 10^{-4}–10^{-6} S cm^{-1} at 300 K, respectively). Hence, LTO is mostly attractive for high-power applications, mainly for HEVs.

To help boost the electrochemical properties of LTO, nanotechnology has been employed in three fronts: (1) use of LTO nanostructures[69], (2) coating of LTO particle surfaces[52,70] and (3) mixing LTO nanostructures with a matrix of conductive materials[71]. Using LTO nanostructures in anodes significantly reduces the Li-ion diffusion pathway within particles and also increases the exposed active electrode area to the electrolyte, both advantageous aspects to achieve high operating currents. In recent years, there have been many attempts to design efficient nanostructures (nanowires[72], nanoflowers[73] and a mesoporous nest-like structure[74]) by adopting new synthetic methods or optimizing existing ones (solvothermal synthesis[75], molten-salt synthesis[76] and microwave irradiation solid-state reaction[77]). These synthetic approaches are usually accompanied by multivalent ion doping to further increase the electronic conductivity of LTO.

Surface coating facilitates the interfacial charge transfer between the LTO and the electrolyte, enhancing the battery power density. Many of the coating materials reported for the graphite anode have also been investigated in the case of LTO, including Ag, Cu, C, SnO_2 and conductive organic compounds. Finally, processing LTO paste with conductive nanomaterials has been shown to improve the low conductivity issue. The conductive matrix accommodates individual LTO particles, which would otherwise be insulating, providing efficient electron-transfer pathways[78] (Fig. 4).

Besides LTO, the family of TiO_2 polymorphs, including anatase, bronze (TiO_2–B), rutile and brookite phases, have also been explored as anodes for LIBs[79]. The lithium insertion/de-insertion is accompanied by the $Ti^{IV} \leftrightarrow Ti^{III}$ redox reaction: $x\mathrm{Li}^+ + \mathrm{TiO}_2 + xe^- \leftrightarrow \mathrm{Li}_x\mathrm{TiO}_2$. Similar to LTO, the low electronic and ionic conductivities of TiO_2 prevent it from achieving superior electrochemical performance. Therefore, similar nanoengineering strategies have also been widely applied for these anode materials[80]. However, it should be pointed out that commercial application of TiO_2 polymorphs in plug-in HEVs has been limited due to the relatively higher cost than LTO.

Improving energy density using silicon nanocomposites. Silicon has drawn much attention as an anode material[44,81–88], because it offers a theoretical capacity of 3572 mAh g^{-1}, more than one order magnitude higher than graphite and LTO. Elemental Si reacts with Li via an alloy/de-alloy mechanism, forming binary Li–Si alloys. However, a volumetric change of more than 300% during battery cycling causes repeated expansion and contraction in the anode structure, leading to particle cracking and active material isolation, which ultimately results in a rapid reversible capacity loss.

In general, Si nanoparticles perform better than films and microparticles in LIBs, because they have better tolerance to mechanical stress. Therefore, several examples of Si nanostructures for anodes in LIBs have appeared in the literature[83,89,90], including 1D Si nanowires and nanotubes[91–94]. With good electronic contact between the Si nanostructures, the current collector and electrolyte, the reversible capacity of those devices can reach as high as 2,000 mAh g^{-1} with good cyclability. More complex hierarchical structures made of Si–C composites have also been reported[95], where Si nanoparticles are uniformly deposited on carbon-black dendritic backbones. In such architectures, both the Si and graphitic carbon are active components; carbon, in particular plays multiple roles: as a conductive matrix for more efficient charge transfer, as a buffer to accommodate the Si volume change and as an active Li-ion host for reversible capacity. These structures can reach a reversible capacity of 1,950 mAh g^{-1} (ref. 96).

In terms of fabrication, CVD and other deposition techniques[97] have been used to improve the performances of Si nanostructures for LIBs. Although these studies can provide valuable insights, such vacuum deposition strategies are less applicable in large-scale commercial settings due to their high cost.

Wet-chemistry synthesis of Si–C nanocomposites provides a more realistic, low-cost alternative for industrial production[98,99]. To this end, hydro-/solvothermal preparation of Si–C nanostructures has been actively pursued, as well as supercritical-fluid-liquid growth for Si nanowires[99]. By coating these Si nanowires with C, an overall reversible capacity of 1,500 mAh g^{-1} was achieved. Another alternative is the use of commercial Si nanopowder to make secondary Si–C nanostructures[100]. Si nanoparticles are encapsulated in carbon shells forming voids that allow for volume expansion during lithiation. These carbon nanoparticles are then assembled into larger secondary microspheres (an architecture resembling a pomegranate; Fig. 5). This design not only solves the volume change issue, but also provides a stable and spatially confined SEI between the active Si material and electrolyte, leading to very stable cycling (up to 1,000 cycles) at a specific capacity of ~1,200 mAh g^{-1}. Though all these nanodesign efforts are worthwhile, it should be pointed out that from an engineering perspective, it may be difficult to fabricate very thin electrodes at low cost to match the thickness of the current cathode (<200 mAh g^{-1}), a drawback that could limit practical applications.

Other anode materials. There are many other candidates that have been investigated as potential anodes for LIBs, including low-dimension carbon (graphene, carbon nanotubes and hard carbon), metal

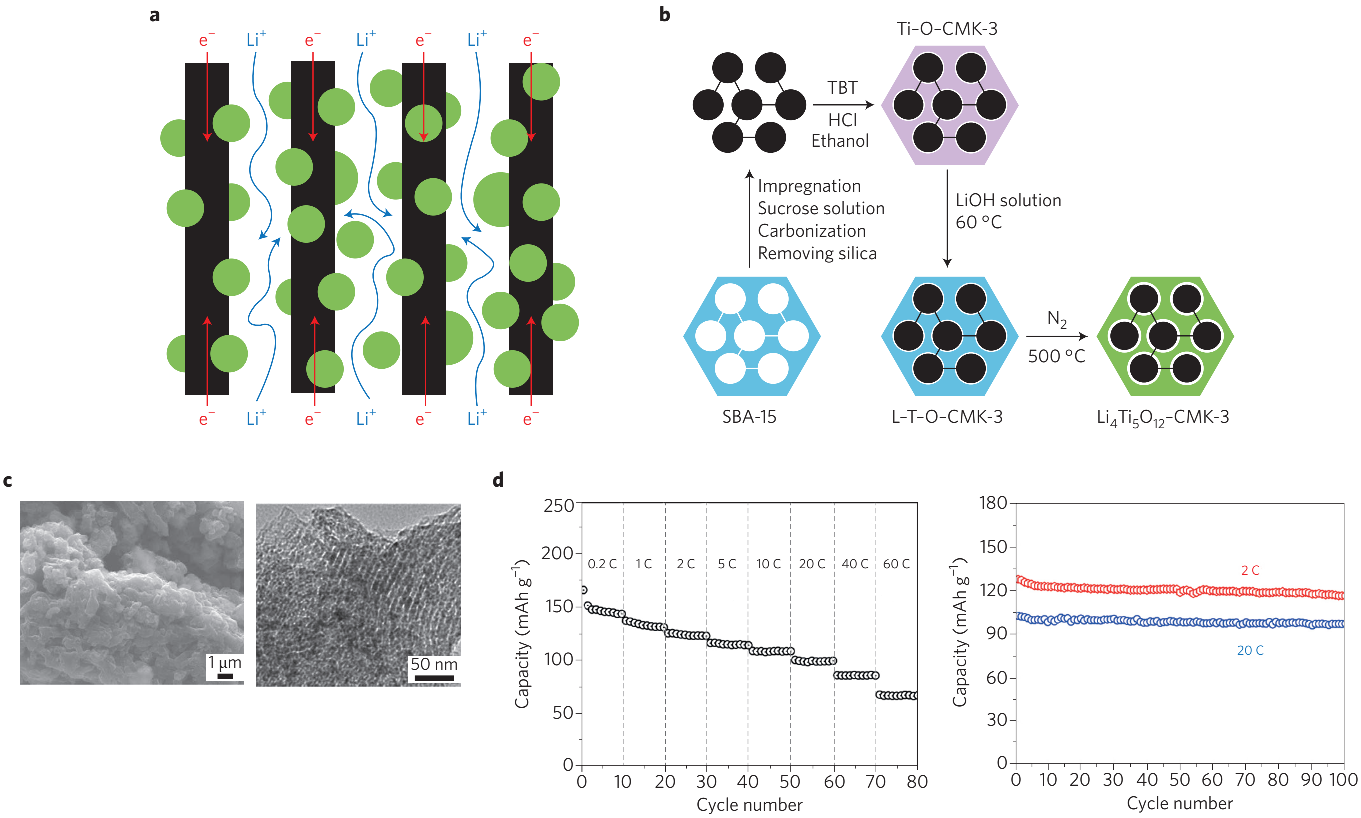

Figure 4 | The lithium titanate-carbon nanocomposites as anodes for LIBs. a, Schematic of the kinetics of Li and electron transport in an ordered mesoporous, micro-/nanosized TiO_2/C composite. Green spheres, TiO_2 nanoparticles; black rods, mesopore carbon matrix. **b**, Synthetic strategy for preparing LTO–carbon mesoporous nanostructures. The ordered mesoporous carbon CMK-3 was synthesized using SBA-15 as a template and sucrose as a carbon source. Then, tetrabutyl titanate (TBT) was converted into a TiO_2 network by hydrolysis in HCl and a heat treatment at 400 °C. The TiO_2 was transformed into $Li_4Ti_5O_{12}$ by chemical lithiation and a short post-annealing procedure to form highly conductive mesoporous, micro-/nanosized TiO_2/C composite . **c**, Scanning electron microscopy (left) and transmission electron microscopy (right) images of the LTO–carbon nanocomposites. **d**, Battery capacity under various cycling conditions. Panels adapted or reproduced from ref. 78, American Chemical Society.

oxides (SnO_2, Co_3O_4 and Sb_2O_3), metal nitrides ($LiMoN_2$) and metal sulfides (FeS_2, NiS_2 and MoS_2). Various nanotechnologies have been actively applied in tailoring these materials for better electrochemical performance in LIBs. The strategies employed are overall similar to what have been used in other anode materials: (1) designing nanostructures for high surface area and better lithium-ion diffusion, (2) nanocoatings to prevent side reactions with electrolytes and (3) mixing with conductive supports to make nanocomposites with enhanced electronic conductivity. It should be noted, however, that these types of anode materials are less likely to be commercialized for EV application in the near term, mainly due to the large, irreversible capacity loss (usually between 30 and 50%) during the initial cycles.

Among all anode materials for LIBs, metallic lithium is certainly the most desired candidate due to a theoretical capacity of about 3,860 mAh g^{-1} (ref. 101). However, the uncontrollable dendritic Li growth during cycling has stood as a huge challenge that has prevented its application for decades. Numerous research efforts have been devoted to stabilizing the Li anode for LIBs[102]. For instance, multilayer graphene coating on Li showed significant performance enhancement[103]. Without doubt, enabling the use of Li metal will significantly boost the energy density of LIBs. Nanotechnology can play a critical role to address the dendrite growth issue.

Although efforts on protecting the Li-metal anode have made significant progress in research labs, challenges still remain before it can be commercialized and become an integral part of the global energy supply chain. In large-scale production, performance, safety and cost are the key concerns. Besides concerns on fabrication costs, it is still unclear whether similar performance and safety can be achieved on pouch cells, as they contain much more active materials when compared with lab coin cells.

Beyond Li-ion technologies

Although lithium intercalation-based batteries have shown significant performance enhancement over the years, they have limitations to the capacities that can be achieved. Therefore, there has been significant effort to develop energy storage technologies beyond Li ion[3,104]. Batteries based on chemical transformations store energy in chemical bonds, such as Li–S and Li–O (ref. 4) and can achieve high energy density and are predicted to be a low-cost technology due to the abundance of sulfur and oxygen. In this section, we review how nanotechnology is playing a key role in enabling this type of batteries. Of the two, batteries based on sulfur are the furthest along in development.

Li–S. Lithium–sulfur batteries exploit the energy stored in Li–S bonds[4,105–107] and can achieve specific capacity on the order of 800 mAh g^{-1} S (against a theoretical capacity of 1,672 mAh g^{-1} S). A Li–S cell is composed of a lithium anode, an organic electrolyte and a sulfur composite cathode. The discharge reaction involves reduction of sulfur by electrons and lithium cations to produce lithium sulfides. The major issue in a Li–S battery is low cyclability owing to the high electronic resistance of sulfur and lithium sulfide products, dissolution of the polysulfides during operation and morphological changes that tend to passivate the cathode. Various strategies based on composite nanomaterials are being explored to mitigate these issues. Although

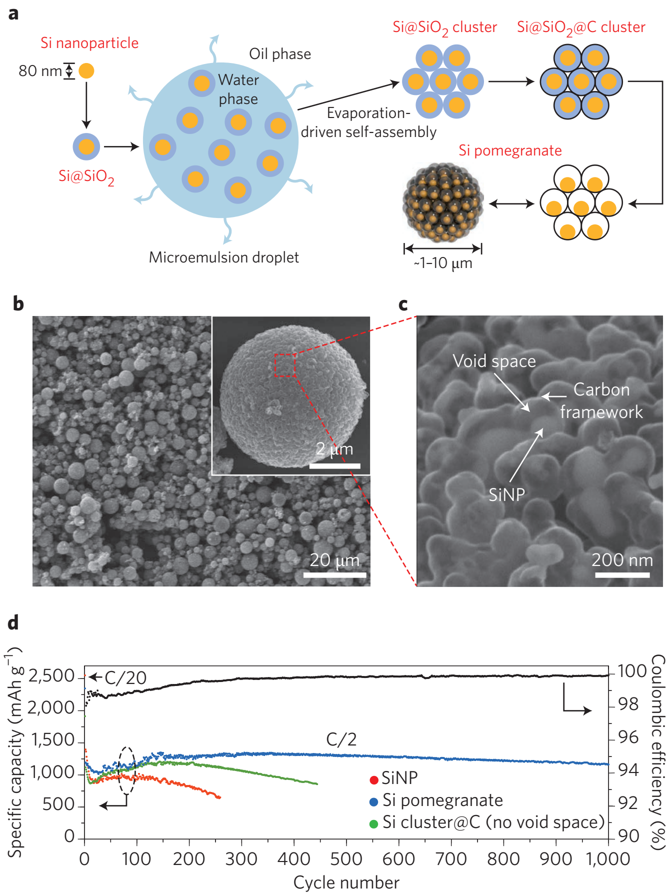

Figure 5 | The 'pomegranate'-structured Si–C nanocomposites as anodes for LIBs. a, The synthetic strategy. Commercial silicon nanoparticles were first coated with a SiO_2 layer using tetraethoxysilane. The aqueous dispersion of Si@SiO_2 nanoparticles was then mixed with 1-octadecene containing 0.3 wt% emulsifier to form water-in-oil emulsions. After evaporation of water, a step-growth polymerization generated a resorcinol-formaldehyde resin layer to wrap the cluster, which was converted into a carbon layer under heat treatment. Finally, the SiO_2 sacrificial layer was removed. **b**, The scanning electron microscopy-imaged morphology of the Si-C core-shell nanoparticles. **c**, Magnified scanning electron microscopy image showing the local structure of silicon nanoparticles and the conductive carbon framework with well-defined void space between. **d**, The reversible delithiation capacity for the first 1,000 galvanostatic cycles of the silicon pomegranate, Si clusters coated on carbon (Si cluster@C) and Si nanoparticles under the same conditions. Panels **a**–**c** reproduced from ref. 100, NPG.

Li–S batteries with up to 1,500 cycles have been demonstrated, they are not yet to the point of commercialization for EVs.

Conventional cathodes for Li–S batteries are made of either sulfur–carbon or sulfur–polymer composites, where the carbon or polymer are added to enhance electronic conductivity and utilization of active materials. Approaches based on nanoporous architectures have been used to immobilize lithium sulfides to address the polysulfide dissolution problem, as well as enhance electronic conductivity. Architectures with pore size smaller than 2 nm have been synthesized from a mixture of sublimed sulfur and microporous carbon spheres[108]. This microporous sulfur–carbon composite constrained electrochemical reactions inside the narrow microporous carbon due to strong adsorption and thus has achieved more than 500 cycles with a capacity of around 800 mAh g^{-1} S. Mesoporous carbon structures (2–50 nm) can provide higher sulfur loading as well as electrical contact and larger capacities[109]. Hierarchical composites of microporous and mesoporous carbons can take advantage of the properties of both materials in one architecture, that is, constraining electrochemical reactions and providing essential electrical contact to the insulating sulfur/sulfides. An example of this type of architecture is the CMK-3 ordered mesoporous carbon that has high sulfur utilization resulting from complete redox activity enabled by electrochemical reactions in the nanosized pores, achieving a high specific capacity of 1,100 mAh g^{-1} S (ref. 110).

However, the above architectures still have problems with polysulfide dissolution. Sulfur composites of porous hollow carbon or metal oxide (such as TiO_2) nanospheres have recently shown promising results in this front[111]. The spheres contain a large hollow inner space that stabilizes the sulfur in a conductive carbon shell, which can also supply Li^+. This type of architecture has led to high capacity retention (up to 1,000 cycles). Another promising architecture involves sulfur–graphene oxide nanocomposites[112,113]. Graphene oxide is an attractive option because it is highly conductive and offers the possibility to modulate its composition through different functional groups. A cycle life of over 1,500 cycles has been achieved in these systems with little capacity fade.

Li–O_2. Compared with Li–S batteries, Li–O_2 cells are in the early research stage of development. The main challenges, here, are: charge overpotentials, electrolyte stability and poor cycle life[5]. The non-aqueous Li–O_2 battery is composed of a lithium anode, an organic electrolyte and a carbon cathode with a theoretical energy density as high as 3,623 Wh kg^{-1} (considering Li_2O_2 as the discharge product). The discharge reaction involves reduction of oxygen molecule by electrons and reaction with lithium cations to produce lithium peroxide or possibly lithium superoxide. Nanostructured materials have played an important role in the development of Li–O_2 batteries[114]. The cathode is usually composed of nanoporous carbon for delivery of the oxygen to the cell. Catalysts play an important role in both oxygen reduction (discharge) and oxygen evolution (charge) reactions. Metal and metal oxide nanoparticles have been found to be good catalysts and recent results have shown that they can lead to reduced charge overpotentials and efficiencies as high as 90% (ref. 115). Cycle life, however, still remains a key challenge for Li–O_2 batteries.

Perspective

Advances in Li-ion batteries and beyond is likely to continue to be strongly based on innovations from nanotechnology. We expect that the rational design of nanomaterials will play a crucial role in the development of high-energy-density Li-ion batteries, eventually enabling long-range EVs.

An immediate challenge is to reduce the particle size of already intrinsically safe electrode materials, such as $LiFePO_4$ and $Li_4Ti_5O_{12}$, to greatly improve the transport properties of Li ions and electrons. In the case of anodes such as Si-based alloys or oxides, which are generally working outside of the thermodynamic window of current non-aqueous electrolytes, the challenge is to find ways to significantly reduce the rate of parasitic reactions between the charged electrode materials. This can be done by reducing the electrochemically reactive surface area that is directly exposed to the non-aqueous electrolytes. In particular, new nanostructures that can accommodate the large volumetric change during charge/discharge and nanocoating that can address the lack of stable solid-electrolyte interphase are critical aspects for EV applications.

Finally, Li–S and Li–O_2 technologies need the use of lithium metal as the anode material. In turn, this requires stabilization of the lithium/electrolyte interface to reduce parasitic reaction between lithium and the electrolyte and to eliminate the formation of lithium dendrites. On the cathode side, efficient confinement of poor electronic conductors such as Li_2S or Li_2O_2, in nanoporous materials is desired to improve the round trip energy efficiency and cycle life.

Received 27 January 2016; accepted 12 September 2016; published online 6 December 2016

References

1. Dunn, B., Kamath, H. & Tarascon, J. M. Electrical energy storage for the grid: a battery of choices. *Science* **334,** 928–935 (2011).
2. Etacheri, V., Marom, R., Elazari, R., Salitra, G. & Aurbach, D. Challenges in the development of advanced Li-ion batteries: a review. *Energy. Environ. Sci.* **4,** 3243–3262 (2011).
3. Goodenough, J. B. & Park, K.-S. The Li-ion rechargeable battery: a perspective. *J. Am. Chem. Soc.* **135,** 1167–1176 (2013).
4. Bruce, P. G., Freunberger, S. A., Hardwick, L. J. & Tarascon, J.-M. Li–O_2 and Li–S batteries with high energy storage. *Nat. Mater.* **11,** 19–29 (2012).
5. Lu, J. *et al.* Aprotic and aqueous Li–O_2 batteries. *Chem. Rev.* **114,** 5611–5640 (2014).
6. Chen, Z., Lu, Z. & Dahn, J. R. Staging phase transitions in Li_xCoO_2. *J. Electrochem. Soc.* **149,** A1604–A1609 (2002).
7. Padhi, A. K., Nanjundaswamy, K. S. & Goodenough, J. B. Phospho-olivines as positive-electrode materials for rechargeable lithium batteries. *J. Electrochem. Soc.* **144,** 1188–1194 (1997).
8. Chung, S. Y., Bloking, J. T. & Chiang, Y. M. Electronically conductive phospho-olivines as lithium storage electrodes. *Nat. Mater.* **1,** 123–128 (2002).
9. Malik, R., Zhou, F. & Ceder, G. Kinetics of non-equilibrium lithium incorporation in $LiFePO_4$. *Nat. Mater.* **10,** 587–590 (2011).
10. Zhang, K. *et al.* Conformal coating strategy comprising N-doped carbon and conventional graphene for achieving ultrahigh power and cyclability of $LiFePO_4$. *Nano Lett.* **15,** 6756–6763 (2015).
11. Lepage, D., Michot, C., Liang, G., Gauthier, M. & Schougaard, S. B. A soft chemistry approach to coating of $LiFePO_4$ with a conducting polymer. *Angew. Chem. Int. Ed.* **50,** 6884–6887 (2011).
12. Hu, C. *et al.* Suppressing Li_3PO_4 impurity formation in $LiFePO_4/Fe_2P$ by a nonstoichiometry synthesis and its effect on electrochemical properties. *Mater. Lett.* **65,** 1323–1326 (2011).
13. Herle, P. S., Ellis, B., Coombs, N. & Nazar, L. F. Nano-network electronic conduction in iron and nickel olivine phosphates. *Nat. Mater.* **3,** 147–152 (2004).
14. Zhang, P. X. *et al.* First-principles study on the electronic structure of a $LiFePO_4$ (010) surface adsorbed with carbon. *J. Alloys Compd.* **540,** 121–126 (2012).
15. Nishimura, S.-i. *et al.* Experimental visualization of lithium diffusion in Li_xFePO_4. *Nat. Mater.* **7,** 707–711 (2008).
16. Malik, R., Burch, D., Bazant, M. & Ceder, G. Particle size dependence of the ionic diffusivity. *Nano Lett.* **10,** 4123–4127 (2010).
17. Yuan, A., Tian, L., Xu, W. & Wang, Y. Al-doped spinel $LiAl_{0.1}Mn_{1.9}O_4$ with improved high-rate cyclability in aqueous electrolyte. *J. Power Sources* **195,** 5032–5038 (2010).
18. Shkrob, I. A. *et al.* Manganese in graphite anode and capacity fade in Li ion batteries. *J. Phys. Chem. C* **118,** 24335–24348 (2014).
19. Kumagai, N., Komaba, S., Kataoka, Y. & Koyanagi, M. Electrochemical behavior of graphite electrode for lithium ion batteries in Mn and Co additive electrolytes. *Chem. Lett.* **29,** 1154–1155 (2000).
20. Lin, Y.-M. *et al.* Enhanced high-rate cycling stability of $LiMn_2O_4$ cathode by ZrO_2 coating for Li-ion battery. *J. Electrochem. Soc.* **152,** A1526–A1532 (2005).
21. Kim, J.-S. *et al.* The electrochemical stability of spinel electrodes coated with ZrO_2, Al_2O_3, and SiO_2 from colloidal suspensions. *J. Electrochem. Soc.* **151,** A1755–A1761 (2004).
22. Lu, J. *et al.* Effectively suppressing dissolution of manganese from spinel lithium manganate via a nanoscale surface-doping approach. *Nat. Commun.* **5,** 5693 (2014).
23. Yao, J., Shen, C., Zhang, P., Gregory, D. & Wang, L. Surface coating of $LiMn_2O_4$ spinel via *in situ* hydrolysis route: effect of the solution. *Ionics* **19,** 739–745 (2013).
24. Liu, Y., Lv, J., Fei, Y., Huo, X. & Zhu, Y. Improvement of storage performance of $LiMn_2O_4$/graphite battery with AlF_3-coated $LiMn_2O_4$. *Ionics* **19,** 1241–1246 (2013).
25. Komaba, S. *et al.* Impact of 2-vinylpyridine as electrolyte additive on surface and electrochemistry of graphite for C/$LiMn_2O_4$ Li-ion cells. *J. Electrochem. Soc.* **152,** A937–A946 (2005).
26. Zhan, C., Qiu, X., Lu, J. & Amine, K. Tuning the Mn deposition on the anode to improve the cycle performance of the Mn-based lithium ion battery. *Adv. Mater. Interfaces* **3,** 1500856 (2016).
27. Sun, Y.-K. *et al.* The role of AlF_3 coatings in improving electrochemical cycling of Li-enriched nickel-manganese oxide electrodes for Li-ion batteries. *Adv. Mater.* **24,** 1192–1196 (2012).
28. Chebiam, R. V., Kannan, A. M., Prado, F. & Manthiram, A. Comparison of the chemical stability of the high energy density cathodes of lithium-ion batteries. *Electrochem. Commun.* **3,** 624–627 (2001).
29. Liu, L. & Chen, X. Titanium dioxide nanomaterials: self-structural modifications. *Chem. Rev.* **114,** 9890–9918 (2014).
30. Chen, Z., Qin, Y., Amine, K. & Sun, Y. K. Role of surface coating on cathode materials for lithium-ion batteries. *J. Mater. Chem.* **20,** 7606–7612 (2010).
31. Cho, J., Kim, Y. W., Kim, B., Lee, J. G. & Park, B. A breakthrough in the safety of lithium secondary batteries by coating the cathode material with $AlPO_4$ nanoparticles. *Angew. Chem. Int. Ed.* **42,** 1618–1621 (2003).
32. Chen, Z. & Dahn, J. R. Methods to obtain excellent capacity retention in $LiCoO_2$ cycled to 4.5 V. *Electrochim. Acta* **49,** 1079–1090 (2004).
33. Meng, X., Yang, X.-Q. & Sun, X. Emerging applications of atomic layer deposition for lithium-ion battery studies. *Adv. Mater.* **24,** 3589–3615 (2012).
34. Sun, Y.-K., Myung, S.-T., Kim, M.-H., Prakash, J. & Amine, K. Synthesis and characterization of $Li[(Ni_{0.8}Co_{0.1}Mn_{0.1})_{0.8}(Ni_{0.5}Mn_{0.5})_{0.2}]O_2$ with the microscale core–shell structure as the positive electrode material for lithium batteries. *J. Am. Chem. Soc.* **127,** 13411–13418 (2005).
35. Sun, Y. K. *et al.* Nanostructured high-energy cathode materials for advanced lithium batteries. *Nat. Mater.* **11,** 942–947 (2012).
36. Noh, H.-J. *et al.* Cathode material with nanorod structure — an application for advanced high-energy and safe lithium batteries. *Chem. Mater.* **25,** 2109–2115 (2013).
37. Xu, M. *et al.* Tris (pentafluorophenyl) phosphine: an electrolyte additive for high voltage Li-ion batteries. *Electrochem. Commun.* **18,** 123–126 (2012).
38. Abe, K., Ushigoe, Y., Yoshitake, H. & Yoshio, M. Functional electrolytes: novel type additives for cathode materials, providing high cycleability performance. *J. Power Sources* **153,** 328–335 (2006).
39. Tarnopolskiy, V. *et al.* Beneficial influence of succinic anhydride as electrolyte additive on the self-discharge of 5 V $LiNi_{0.4}Mn_{1.6}O_4$ cathodes. *J. Power Sources* **236,** 39–46 (2013).
40. von Cresce, A. & Xu, K. Electrolyte additive in support of 5 V Li ion chemistry. *J. Electrochem. Soc.* **158,** A337–A342 (2011).
41. Winter, M., Besenhard, J. O., Spahr, M. E. & Novák, P. Insertion electrode materials for rechargeable lithium batteries. *Adv. Mater.* **10,** 725–763 (1998).
42. Dahn, J. *et al.* in *Lithium Batteries: New Materials, Developments, and Perspectives* (ed. Pistoria, G.) Ch. 1 (Elsevier, 1994).
43. Ohzuku, T., Ueda, A. & Yamamoto, N. Zero-strain insertion material of $Li[Li_{1/3}Ti_{5/3}]O_4$ for rechargeable lithium cells. *J. Electrochem. Soc.* **142,** 1431–1435 (1995).
44. Park, C.-M., Kim, J.-H., Kim, H. & Sohn, H.-J. Li-alloy based anode materials for Li secondary batteries. *Chem. Soc. Rev.* **39,** 3115–3141 (2010).
45. Reddy, M., Subba Rao, G. & Chowdari, B. Metal oxides and oxysalts as anode materials for Li ion batteries. *Chem. Rev.* **113,** 5364–5457 (2013).
46. Endo, M., Kim, C., Nishimura, K., Fujino, T. & Miyashita, K. Recent development of carbon materials for Li ion batteries. *Carbon* **38,** 183–197 (2000).
47. Buqa, H., Goers, D., Holzapfel, M., Spahr, M. E. & Novák, P. High rate capability of graphite negative electrodes for lithium-ion batteries. *J. Electrochem. Soc.* **152,** A474–A481 (2005).
48. Aurbach, D., Markovsky, B., Weissman, I., Levi, E. & Ein-Eli, Y. On the correlation between surface chemistry and performance of graphite negative electrodes for Li ion batteries. *Electrochim. Acta* **45,** 67–86 (1999).
49. Smart, M. C. *et al.* Irreversible capacities of graphite in low-temperature electrolytes for lithium-ion batteries. *J. Electrochem. Soc.* **146,** 3963–3969 (1999).
50. Jeong, S.-K., Inaba, M., Abe, T. & Ogumi, Z. Surface film formation on graphite negative electrode in lithium-ion batteries: AFM study in an ethylene carbonate-based solution. *J. Electrochem. Soc.* **148,** A989–A993 (2001).
51. Kulova, T. L. *et al.* Electrochemical characteristics of negative electrodes made of ozone-treated graphite for lithium-ion batteries. *Russ. J. Electrochem.* **37,** 1017–1023 (2001).
52. Li, H. & Zhou, H. Enhancing the performances of Li-ion batteries by carbon-coating: present and future. *Chem. Commun.* **48,** 1201–1217 (2012).
53. Yoshio, M., Wang, H., Fukuda, K., Hara, Y. & Adachi, Y. Effect of carbon coating on electrochemical performance of treated natural graphite as lithium-ion battery anode material. *J. Electrochem. Soc.* **147,** 1245–1250 (2000).
54. Yoshio, M., Wang, H. & Fukuda, K. Spherical carbon-coated natural graphite as a lithium-ion battery-anode material. *Angew. Chem. Int. Ed.* **42,** 4203–4206 (2003).
55. Yoshio, M. *et al.* Improvement of natural graphite as a lithium-ion battery anode material, from raw flake to carbon-coated sphere. *J. Mater. Chem.* **14,** 1754–1758 (2004).
56. Gao, J. *et al.* Suppression of PC decomposition at the surface of graphitic carbon by Cu coating. *Electrochem. Commun.* **8,** 1726–1730 (2006).
57. Yang, L. C., Guo, W. L., Shi, Y. & Wu, Y. P. Graphite@MoO_3 composite as anode material for lithium ion battery in propylene carbonate-based electrolyte. *J. Alloys Compd.* **501,** 218–220 (2010).
58. Guo, K., Pan, Q. & Fang, S. Poly(acrylonitrile) encapsulated graphite as anode materials for lithium ion batteries. *J. Power Sources* **111,** 350–356 (2002).
59. Zhang, H.-L. *et al.* Electrochemical performance of pyrolytic carbon-coated natural graphite spheres. *Carbon* **44,** 2212–2218 (2006).
60. Park, G., Gunawardhana, N., Nakamura, H., Lee, Y. & Yoshio, M. Suppression of Li deposition on surface of graphite using carbon coating by thermal vapor deposition process. *J. Power Sources* **196,** 9820–9824 (2011).

61. Nozaki, H., Nagaoka, K., Hoshi, K., Ohta, N. & Inagaki, M. Carbon-coated graphite for anode of lithium ion rechargeable batteries: carbon coating conditions and precursors. *J. Power Sources* **194,** 486–493 (2009).
62. Ding, Y.-S. *et al.* Characteristics of graphite anode modified by CVD carbon coating. *Surf. Coat. Technol.* **200,** 3041–3048 (2006).
63. Lee, M.-L. *et al.* Atomic layer deposition of TiO_2 on negative electrode for lithium ion batteries. *J. Power Sources* **244,** 410–416 (2013).
64. Lu, W., Donepudi, V. S., Prakash, J., Liu, J. & Amine, K. Electrochemical and thermal behavior of copper coated type MAG-20 natural graphite. *Electrochim. Acta* **47,** 1601–1606 (2002).
65. Pan, Q., Guo, K., Wang, L. & Fang, S. Novel modified graphite as anode material for lithium-ion batteries. *J. Electrochem. Soc.* **149,** A1218–A1223 (2002).
66. Veeraraghavan, B., Paul, J., Haran, B. & Popov, B. Study of polypyrrole graphite composite as anode material for secondary lithium-ion batteries. *J. Power Sources* **109,** 377–387 (2002).
67. Zhang, H.-L., Li, F., Liu, C. & Cheng, H.-M. Poly(vinyl chloride) (PVC) coated idea revisited: influence of carbonization procedures on PVC-coated natural graphite as anode materials for lithium ion batteries. *J. Phys. Chem. C* **112,** 7767–7772 (2008).
68. Ouyang, C. Y., Zhong, Z. Y. & Lei, M. S. *Ab initio* studies of structural and electronic properties of $Li_4Ti_5O_{12}$ spinel. *Electrochem. Commun.* **9,** 1107–1112 (2007).
69. Prakash, A. S. *et al.* Solution-combustion synthesized nanocrystalline $Li_4Ti_5O_{12}$ as high-rate performance Li-ion battery anode. *Chem. Mater.* **22,** 2857–2863 (2010).
70. Rahman, M. M., Wang, J.-Z., Hassan, M. F., Wexler, D. & Liu, H. K. Amorphous carbon coated high grain boundary density dual phase $Li_4Ti_5O_{12}$-TiO_2: a nanocomposite anode material for Li-ion batteries. *Adv. Energy Mater.* **1,** 212–220 (2011).
71. Kim, H.-K., Bak, S.-M. & Kim, K.-B. $Li_4Ti_5O_{12}$/reduced graphite oxide nano-hybrid material for high rate lithium-ion batteries. *Electrochem. Commun.* **12,** 1768–1771 (2010).
72. Shen, L., Uchaker, E., Zhang, X. & Cao, G. Hydrogenated $Li_4Ti_5O_{12}$ nanowire arrays for high rate lithium ion batteries. *Adv. Mater.* **24,** 6502–6506 (2012).
73. Chiu, H.-c. & Demopoulos, G. P. A novel green approach to synthesis of nanostructured $Li_4Ti_5O_{12}$ anode material. *ECS Trans.* **50,** 119–126 (2013).
74. Chen, J., Yang, L., Fang, S., Hirano, S.-i. & Tachibana, K. Synthesis of hierarchical mesoporous nest-like $Li_4Ti_5O_{12}$ for high-rate lithium ion batteries. *J. Power Sources* **200,** 59–66 (2012).
75. Laumann, A. *et al.* Rapid green continuous flow supercritical synthesis of high performance $Li_4Ti_5O_{12}$ nanocrystals for Li ion battery applications. *J. Electrochem. Soc.* **159,** A166–A171 (2011).
76. Bai, Y., Wang, F., Wu, F., Wu, C. & Bao, L.-y. Influence of composite LiCl–KCl molten salt on microstructure and electrochemical performance of spinel $Li_4Ti_5O_{12}$. *Electrochim. Acta* **54,** 322–327 (2008).
77. Li, J., Jin, Y.-L., Zhang, X.-G. & Yang, H. Microwave solid-state synthesis of spinel $Li_4Ti_5O_{12}$ nanocrystallites as anode material for lithium-ion batteries. *Solid State Ion.* **178,** 1590–1594 (2007).
78. Shen, L. *et al.* Three-dimensional coherent titania–mesoporous carbon nanocomposite and its lithium-ion storage properties. *ACS Appl. Mater. Interfaces* **4,** 2985–2992 (2012).
70. Djenizian, T., Hanzu, I. & Knauth, P. Nanostructured negative electrodes based on titania for Li-ion microbatteries. *J. Mater. Chem.* **21,** 9925–9937 (2011).
80. Liu, H. *et al.* Mesoporous TiO_2–B microspheres with superior rate performance for lithium ion batteries. *Adv. Mater.* **23,** 3450–3454 (2011).
81. Boukamp, B. A., Lesh, G. C. & Huggins, R. A. All-solid lithium electrodes with mixed-conductor matrix. *J. Electrochem. Soc.* **128,** 725–729 (1981).
82. Winter, M. & Besenhard, J. O. Electrochemical lithiation of tin and tin-based intermetallics and composites. *Electrochim. Acta* **45,** 31–50 (1999).
83. Wu, H. & Cui, Y. Designing nanostructured Si anodes for high energy lithium ion batteries. *Nano Today* **7,** 414–429 (2012).
84. Yoshio, M. *et al.* Carbon-coated Si as a lithium-ion battery anode material. *J. Electrochem. Soc.* **149,** A1598–A1603 (2002).
85. Johnson, C. S., Li, N., Lefief, C. & Thackeray, M. M. Anomalous capacity and cycling stability of *x*Li(2)MnO(3)center dot(1–*x*)$LiMO_2$ electrodes (M = Mn, Ni, Co) in lithium batteries at 50 degrees C. *Electrochem. Commun.* **9,** 787–795 (2007).
86. Obrovac, M. N., Christensen, L., Le, D. B. & Dahn, J. R. Alloy design for lithium-ion battery anodes. *J. Electrochem. Soc.* **154,** A849–A855 (2007).
87. Sandu, I., Moreau, P., Guyomard, D., Brousse, T. & Roué, L. Synthesis of nanosized Si particles via a mechanochemical solid–liquid reaction and application in Li-ion batteries. *Solid State Ion.* **178,** 1297–1303 (2007).
88. Phan, V. P., Pecquenard, B. & Le Cras, F. High-performance all-solid-state cells fabricated with silicon electrodes. *Adv. Funct. Mater.* **22,** 2580–2584 (2012).
89. Szczech, J. R. & Jin, S. Nanostructured silicon for high capacity lithium battery anodes. *Energy Environ. Sci.* **4,** 56–72 (2011).
90. Liu, N. *et al.* a yolk-shell design for stabilized and scalable li-ion battery alloy anodes. *Nano Lett.* **12,** 3315–3321 (2012).
91. Chan, C. K. *et al.* High-performance lithium battery anodes using silicon nanowires. *Nat. Nanotech.* **3,** 31–35 (2008).
92. Cui, L.-F., Ruffo, R., Chan, C. K., Peng, H. & Cui, Y. Crystalline-amorphous core–shell silicon nanowires for high capacity and high current battery electrodes. *Nano Lett.* **9,** 491–495 (2009).
93. Hertzberg, B., Alexeev, A. & Yushin, G. Deformations in Si–Li anodes upon electrochemical alloying in nano-confined space. *J. Am. Chem. Soc.* **132,** 8548–8549 (2010).
94. Choi, N.-S., Yao, Y., Cui, Y. & Cho, J. One dimensional Si/Sn-based nanowires and nanotubes for lithium-ion energy storage materials. *J. Mater. Chem.* **21,** 9825–9840 (2011).
95. Ma, H. *et al.* Nest-like silicon nanospheres for high-capacity lithium storage. *Adv. Mater.* **19,** 4067–4070 (2007).
96. Magasinski, A. *et al.* High-performance lithium-ion anodes using a hierarchical bottom-up approach. *Nat. Mater.* **9,** 353–358 (2010).
97. Yin, J. *et al.* Micrometer-scale amorphous Si thin-film electrodes fabricated by electron-beam deposition for Li-ion batteries. *J. Electrochem. Soc.* **153,** A472–A477 (2006).
98. Mazouzi, D., Lestriez, B., Roué, L. & Guyomard, D. Silicon composite electrode with high capacity and long cycle life. *Electrochem. Solid State Lett.* **12,** A215–A218 (2009).
99. Chan, C. K., Patel, R. N., O'Connell, M. J., Korgel, B. A. & Cui, Y. Solution-grown silicon nanowires for lithium-ion battery anodes. *ACS Nano* **4,** 1443–1450 (2010).
100. Liu, N. *et al.* A pomegranate-inspired nanoscale design for large-volume-change lithium battery anodes. *Nat. Nanotech.* **9,** 187–192 (2014).
101. Xu, W. *et al.* Lithium metal anodes for rechargeable batteries. *Energy. Environ. Sci.* **7,** 513–537 (2014).
102. Cheng, X.-B. *et al.* A review of solid electrolyte interphases on lithium metal anode. *Adv. Sci.* **3,** 1500213 (2015).
103. Kim, J.-S., Kim, D. W., Jung, H. T. & Choi, J. W. Controlled lithium dendrite growth by a synergistic effect of multilayered graphene coating and an electrolyte additive. *Chem. Mater.* **27,** 2780–2787 (2015).
104. Van Noorden, R. A better battery. *Nature* **507,** 26–28 (2014).
105. Nazar, L. F., Cuisinier, M. & Pang, Q. Lithium-sulfur batteries. *MRS Bull.* **39,** 436–442 (2014).
106. Manthiram, A., Fu, Y. Z. & Su, Y. S. Challenges and prospects of lithium–sulfur batteries. *Acc. Chem. Res.* **46,** 1125–1134 (2013).
107. Yin, Y. X., Xin, S., Guo, Y. G. & Wan, L. J. Lithium–sulfur batteries: electrochemistry, materials, and prospects. *Angew. Chem. Int. Ed.* **52,** 13186–13200 (2013).
108. Zhang, B., Qin, X., Li, G. R. & Gao, X. P. Enhancement of long stability of sulfur cathode by encapsulating sulfur into micropores of carbon spheres. *Energy. Environ. Sci.* **3,** 1531–1537 (2010).
109. Liang, C. D., Dudney, N. J. & Howe, J. Y. Hierarchically structured sulfur/carbon nanocomposite material for high-energy lithium battery. *Chem. Mater.* **21,** 4724–4730 (2009).
110. Ji, X. L., Lee, K. T. & Nazar, L. F. A highly ordered nanostructured carbon-sulphur cathode for lithium-sulphur batteries. *Nat. Mater.* **8,** 500–506 (2009).
111. Seh, Z. W. *et al.* Sulphur–TiO_2 yolk-shell nanoarchitecture with internal void space for long-cycle lithium-sulphur batteries. *Nat. Commun.* **4,** 1331 (2013).
112. Song, M. K., Zhang, Y. G. & Cairns, E. J. A long-life, high-rate lithium/sulfur cell: a multifaceted approach to enhancing cell performance. *Nano Lett.* **13,** 5891–5899 (2013).
113. Chen, R. J. *et al.* Graphene-based three-dimensional hierarchical sandwich-type architecture for high-performance Li/S batteries. *Nano Lett.* **13,** 4642–4649 (2013).
114. Lu, J. *et al.* A lithium–oxygen battery based on lithium superoxide. *Nature* **529,** 377–382 (2016).
115. Lu, J. *et al.* A nanostructured cathode architecture for low charge overpotential in lithium–oxygen batteries. *Nat. Commun.* **4,** 2383 (2013).

Acknowledgements

This work was supported by the US Department of Energy under Contract DE-AC0206CH11357 with the main support provided by the Vehicle Technologies Office, Department of Energy (DOE) Office of Energy Efficiency and Renewable Energy (EERE). We also acknowledge support from the Chinese Electric Power Research Institute (CEPRI).

Additional information

Correspondence and requests for materials should be addressed to F.P., L.A.C. and K.A.

Competing financial interests

The authors declare no competing financial interests.